



Dual Dielectrically Modulated Electrostatically Doped Tunnel-FET for Biosensing Applications

L.K. Bramhane¹, P.K. Kadbe¹, B.H. Patil¹, S.D. Chede² and S.B. Lande²

¹Assistant Professor, Department of E & TC VPKBIET, Baramati, Pune (Maharashtra), India.

²Professor, Department E & TC VPKBIET, Baramati, Pune (Maharashtra), India.

(Corresponding author: L.K. Bramhane)

(Received 29 August 2019, Revised 25 October 2019, Accepted 04 November 2019)

(Published by Research Trend, Website: www.researchtrend.net)

ABSTRACT: For next-generation biosensing applications, a dual dielectrically modulated tunnel field effect transistor based on electrostatically doping (DDM-EDTFET) has been proposed. The proposed device is implemented with the aim of reducing the fabrication complexity and cost of TFET based biosensor with nanoscale dimensions. For this, the proposed biosensor device utilizes polarity gate concept based on electrostatic doping to form the source-drain region. Moreover, a nanogap cavity is stacked between the gate electrode and HfO₂ layer for detection of target biomolecules. In this pursuit, the proposed biosensor device offers significant sensing performance along with superior doping control over channel with minimum process variability issues and thermal budget. Based on extensive two-D TCAD device level simulations, sensing performance of the proposed biosensor device has been evaluated for both the charged ($k > 1$, $\rho \neq 0$) and charge-neutral ($k > 1$, $\rho = 0$) biomolecules. Furthermore, the sensing capability has been analyzed through distinct dielectric constant (k) and negative charge density (ρ^-) of biomolecule at a specific gate and drain bias conditions.

Keywords: Polarity control, Doping-less, Band-to-band Tunneling (BTBT), Biosensor, Biomolecules, Dielectrically modulated.

Abbreviations: DDM-EDTFET, Dual Dielectrically Modulated Electrostatically Doped Tunnel-Field Effect Transistor; ISFETs, ion-sensitive FETs; DM-FET, dielectric modulated FET; T_{Si} , Silicon Thickness; T_{ox} , Oxide Thickness; ϕ_m , Metal Work function.

I. INTRODUCTION

Biosensors are the strong candidate for their ability to detect the charged molecules as well as the neutral molecules (species). In literature, the electrochemical based biosensors are the strong contender for the supervision of infectious agents due to their high sensitivity and cost effectiveness [1-8]. However, for early-stage electrochemical detection, a highly specific, sensitive, selective and reliable biosensor can play a crucial role due to their ability to convert biological information directly into a processable electrical signal. Moreover, with the combination of surface physics and bioengineering, ion-sensitive FETs (ISFETs) was proposed for the fast detection of charged biomolecules that exist between the dielectric gate and electrolyte solution [5]. However, ISFETs have parasitic sensitivity to temperature and light. Moreover, unable to detect the neutral biomolecules and have the compatibility issue with the CMOS process. In [8-10], to solve the problem of detecting neutral biomolecules and to modulate electrostatic properties, a cavity based dielectric modulated FET (DM-FET) has been proposed. The nanogap cavity can be formed using the process steps reported in [4, 7]. But these devices have low binding probability in carved cavity region [4-6]. However, tunnel FET-based biosensors investigated widely for their superior sensitivity and quick response time when it is compared to biosensors based on FET [1, 2, 11,12]. But, these devices postulate different metals to doped the regions.

Also, ion implantation, annealing for damage removal and dopant activation process make fabrication of these devices complex and expensive. Hence, doping less devices that are based on charge plasma (work function engineering) have been recently proposed to eliminate the requirement of different processes used to doped the targeted regions [13-16]. Although, in these devices, the problem of choosing different work function metal or formation of alloys having a desired work function is still persisting and needed to resolve. Hence, to solve the problem of selecting different work function metals and to increase the ability to detect a species correctly, a way of dealing with the issues needed to optimize further to fulfill the requirements of next-generation biosensing applications [17]. In this paper, DDM-EDTFET is proposed to detect the different types of biomolecules and to resolve the issues of doping requirements and selecting an appropriate metal work function. For this, an electrostatic polarity control doping has been adopted in the proposed DDM-EDTFET in which a positive or negative supply voltage is applied to the polarity control electrodes to induce the charge carriers (electrons or holes) in targeted silicon region. For example, a positive supply voltage applied to polarity control electrode results in an accumulation of electrons while a negative voltage on polarity control electrode accumulates holes.

Moreover, HfO₂ has been introduced between the silicon and cavity region to modulate the electrical properties of the proposed device.

Furthermore, the nanogap cavity on top of or beneath HfO_2 is used to sense both charged and neutral biomolecules. Apart from this, the impact on sensitivity, ON-current, sub-threshold slope, and electron tunneling rate have been studied with variation in density of charged and neutral biomolecules.

II. DEVICE DIMENSIONS AND MODELS

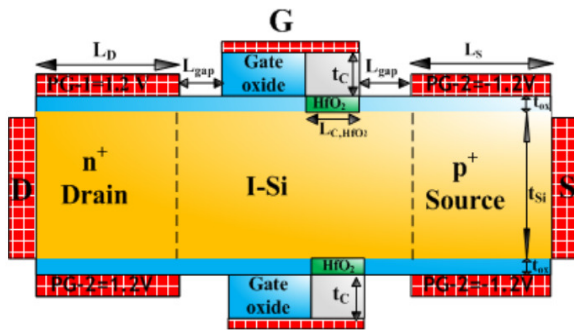


Fig. 1. Cross-sectional structural view of dual dielectrically modulated electrostatically doped tunnel-FET (DDM-EDTFET).

Fig. 1 shows the cutaway view of a DDM-EDTFET structure [12] with embedded nanogap cavity within the gate dielectric towards the source end. The simulation parameters adapted from [12] are silicon film thickness ($T_{\text{Si}} = 10 \text{ nm}$), oxide layer ($T_{\text{ox}} = 1 \text{ nm}$), gate length ($L_g = 50 \text{ nm}$) and Control Gate (CG) metal work function ($= 4.5 \text{ eV}$). The formation of n^+ and p^+ D/S regions in an intrinsic Si film, is achieved through electrostatically doping i.e with the application of appropriate positive (+1.2 V)/negative (-1.2V) bias at polarity gates, PG-1/PG-2, respectively. Silicon thickness is kept within the Debye length for uniform distribution of the charge carrier [17]. Moreover, work functions of all gate electrodes ($\phi_m = 0.45 \text{ eV}$) are compound of nickel silicide (NiSi) [10]. Both spacer lengths are of 5 nm. In Fig. 1, the nanogap cavity formed between the gate electrode and HfO_2 layer and have the same process steps that are described in [2]. To avoid the sensitivity degradation due to gate-to-channel leakage current, a thin layer 1nm of dielectric material (HfO_2 is considered in this work) as an insulator within the nanogap cavity is essential [1]. In the event of biomolecules conjugation within the nanogap cavity under the gate, the gate capacitance increases which in turn, helps in an enhancement in drain current in DDM-EDTFET. The term biomolecule conjugation depicts the variation of biomolecules accumulation when considered a distinct dielectric and/or charge density beneath cavity region [1]. When there is no biomolecule ($k = 1$) i.e. air cavity, there is no formation of channel beneath the HfO_2 layer. However, paralyzed biomolecules in cavity result change in the cavity capacitance and biomolecules having $k > 1$ results in channel inversion. Therefore, the electron concentration rises below the cavity and in this way, magnitude of drain current enhanced [2]. The simulations have been carried out assuming that the nanogap cavity completely occupied by the biomolecules ($k > 1$), and the influence of charged biomolecules ($\rho \neq 0$) is simulated by considering negative charge density at the silicon-oxide interface [18].

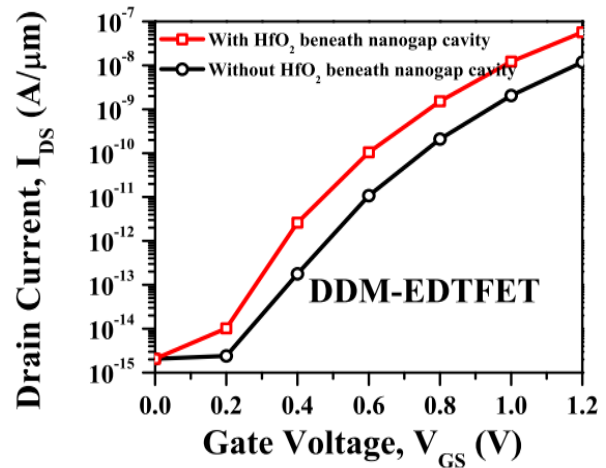


Fig. 2. Transfer characteristics of DDM-EDTFET with and without high-k material, HfO_2 as an insulator in the nanogap cavity filled with biomolecules with dielectric constant, $k=5$ at $V_{\text{DS}} = 1.0 \text{ V}$ and $V_{\text{GS}} = 1.2 \text{ V}$.

III. RESULTS AND DISCUSSION

Atlas Silvaco V5.19.20 [19], a Two-Dimensional device simulator is used to accomplish the parameters of n-channel DDM-EDTFET. However, band-to-band tunneling model, drift-diffusion current transport model, concentration dependent Shockley-Read-Hall (SRH) generation and recombination model are used to extract different parameters. In n channel DDM-EDTFET, the band-to-band tunneling (BTBT) current via junction form between the source and channel is examined under the influence of biomolecule conjugation. The simulations have been carried out as target biomolecules are present in cavity region and keeping consistent difference in between these different values. There are two parameters named dielectric constant and density of charge carrier that can be used for sensitivity analysis of DDM-EDTFET biosensor.

A. Impact of biomolecules conjugation on band profile and surface potential

In this section, primarily, we have shown the influence of biomolecule conjugation on the lateral energy-band profile parallel to the tunneling path. The energy-band profiles in the DDM-EDTFET biosensor for the different values of negative charge densities (ρ^-) as well as dielectric constants (k) of the biomolecules are shown in Fig. 3 (a) and (b), respectively, under the ON-state considering $V_{\text{GS}} = 1.2 \text{ V}$ and $V_{\text{DS}} = 0.5 \text{ V}$ to ensure the noteworthy contributions from both these terminals. From, Fig. 3 (a), it is observed that as dielectric constant increases the band bending enhances, and thereby, reduces the minimum tunneling length or barrier width in the event of biomolecule conjugation.

Moreover, Fig. 3 (b) shows energy band profiles for charged biomolecules i.e. the biomolecules with ρ^- in the cavity. It is observed that with enhancement in ρ^- , the barrier height increases in the nanogap cavity and hence decreasing surface potential and lateral electric field that degrades ON-state current.

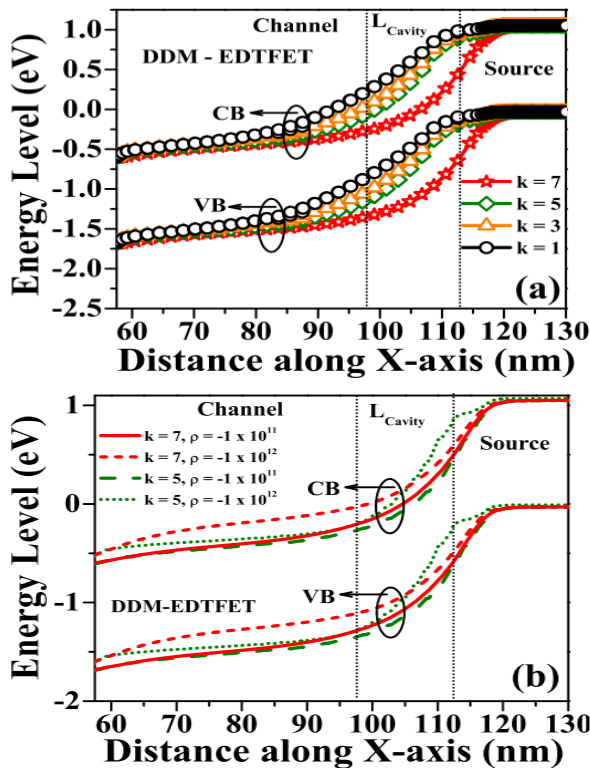


Fig. 3. Energy band diagrams of DDM-EDTFET along the X-axis with distinct values of (a) k when $\rho = 0$ and (b) ρ when $k = 5$ and 7 under ON-state conditions ($V_{DS} = 0.5V$ and $V_{GS} = 1.2V$)

In this regard, we have also shown the impact of biomolecules conjugation with varying dielectric constants and ρ^- on the electron tunneling rate and hence on the ON-state current in Fig. 4 (a) and (b), respectively. The lateral electric field enhances at the tunnel junction due to the presence of biomolecules ($k > 1$) underneath the cavity region, which governs the BTBT generation rate of charge carriers and the tunneling probability. Hence, the generation rate or tunneling rate increases exponentially with the increase in the electric field and leads to an increase in ON-state current of the device as verified from Fig. 4 (a) and (b). Similarly, to investigate the impact of biomolecules conjugation on electrostatic potential of DDM-EDTFET biosensor, we have analyzed the surface potential in ON-state bias condition ($V_{DS} = 0.5V$ and $V_{GS} = 1.2V$) with varying k and ρ^- as shown in Fig. 5 (a) and (b), respectively along the X-axis. It is observed from Fig. 5 (a), that absence of biomolecules ($k=1$) results in minimum surface potential. However as the value of k increases, it reaches to higher values in the presence of biomolecules conjugation ($k > 1$) beneath the nanocavity. This accounts for the fact that the biomolecules with higher values of k enhance the coupling between gate and channel and thereby active capacitance [20]. As a result, the barrier width at the source-channel junction decreases and results in a steep rise in the potential profile underneath the cavity [2]. Similarly, from Fig. 5 (b), effective surface potential decreases when density of negative charge increases. Since, with the negative charge of the biomolecules, the flat band voltage (V_{fb}) is directly proportional to charge density ($e\rho/C$), this, in turn, reduces the effective gate bias ($V_{GS,eff}$), followed by a decrease of the surface potential beneath the

nanogap cavity [2]. However, a low value of charged biomolecules ($\sim 10^{11} \text{ cm}^{-2}$) has negligible impact in comparison with higher charged molecules that cause a significant lowering of the surface potential as confirmed from Fig. 5 (b).

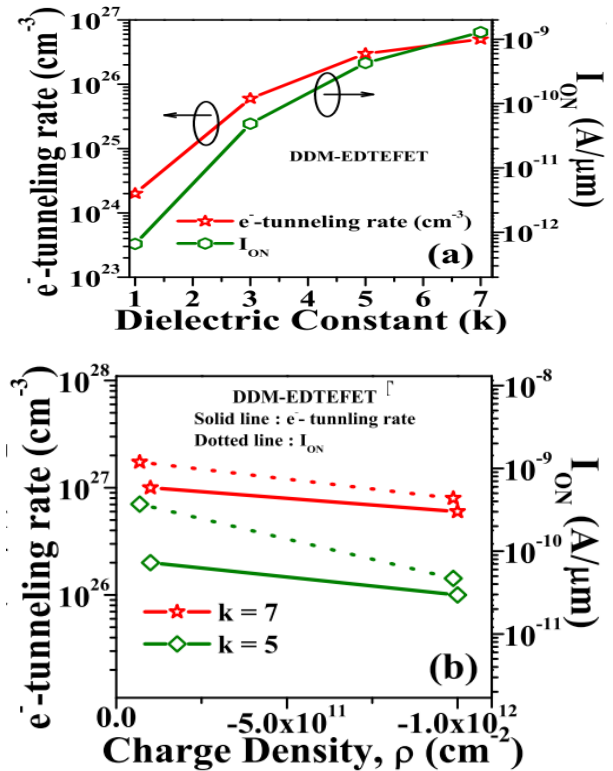


Fig. 4. Electron tunneling rate and ON-state current of DDM-EDTFET with different (a) k when $\rho=0$ and (b) ρ when $k=5$ and 7 under ON-state conditions ($V_{DS} = 0.5V$ and $V_{GS} = 1.2V$).

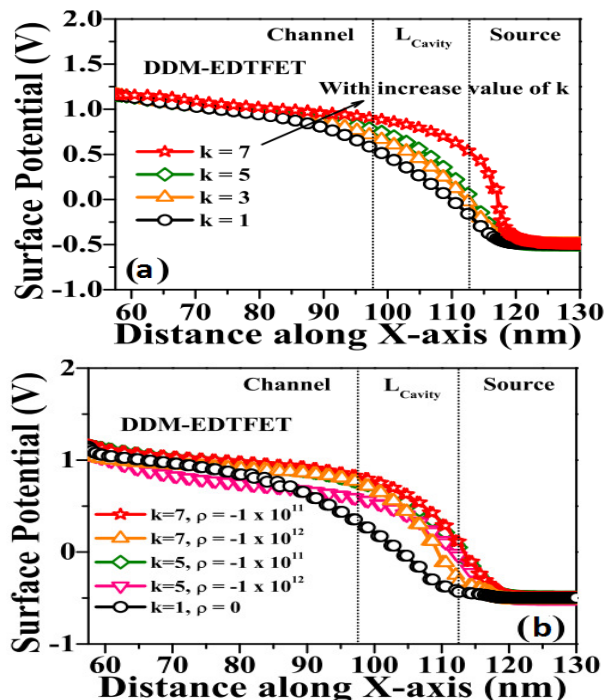


Fig. 5. Surface potential profile of DDM-EDTFET with different (a) k when $\rho=0$ and (b) ρ when $k=5$ and 7 under ON-state conditions ($V_{DS} = 0.5V$ and $V_{GS} = 1.2V$).

B. Impact of biomolecules conjugation on drain current

Fig. 6 shows the transfer characteristics of the DDMEDTFET with varying (a) dielectric constants and (b) negative charge densities in an event of biomolecule conjugation with biasing $V_{GS} = 1.2$ V and $V_{DS} = 1$ V. From Fig. 6 (a), with the value of $k = 1$ (air cavity), it is clear that the DDM-EDTFET exhibits a very low value of ON-state current (10^{-11} A/ μm). As the value of k increases from 1 (presence of biomolecules), then significant improvement in the value of ON-state current is observed. On the other hand, from Fig. 6 (b), an opposite behavior with the increase in the value of negative charge densities in the transfer characteristics of DDM-EDTFET is observed. This is due to the fact that with increase in negative charge densities, the surface potential decreases (Fig. 5 (b)) which causes the degradation in the ON-state current of the device. It is worthwhile to mention that at $k = 7$, DDM-EDTFET attains higher value of ON-State current (10^{-7} A/ μm) with minimum degradation with ρ^- in comparison with $k = 5$ (Fig. 6 (b)). Fig. 7 show the output characteristics of the DDMEDTFET for different values of (a) dielectric constant and (b) negative charge densities. The output characteristics depict the same behavioral changes with respect to variation in dielectric constant and negative charge densities as that shown by the transfer characteristics.

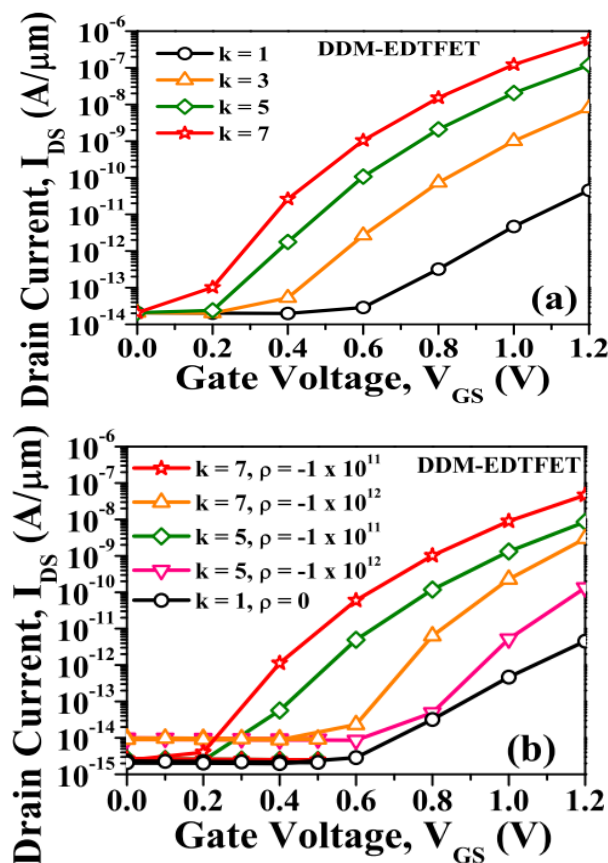


Fig. 6. Transfer characteristics of DDM-EDTFET with different (a) k when $\rho = 0$ and (b) ρ when $k = 5$ and 7 at $V_{GS} = 1.2$ V and $V_{DS} = 1$ V.

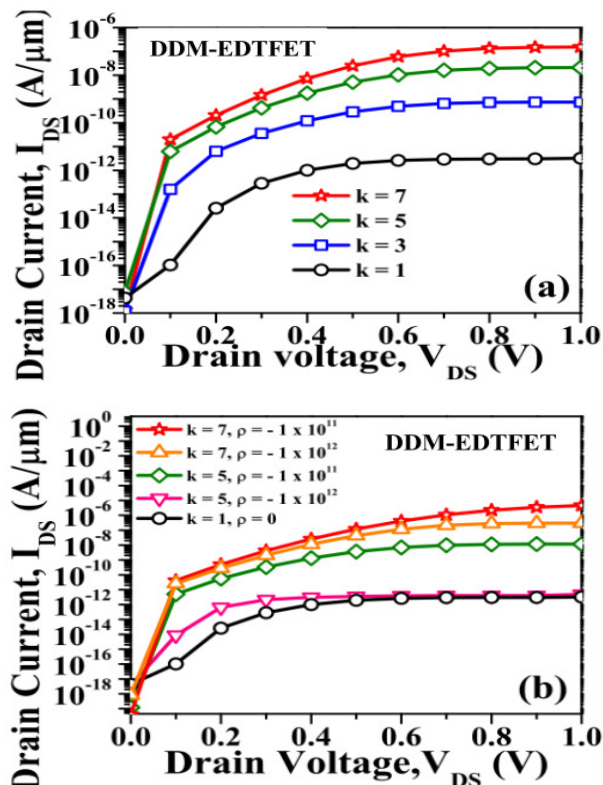


Fig. 7. Output characteristics of DDM-EDTFET with different (a) k when $\rho = 0$ and (b) ρ when $k = 5$ and 7 at $V_{GS} = 0.5$ V and $V_{DS} = 1$ V.

C. Sensitivity analysis with respect to biomolecule conjugation

The effectiveness of the DDM-EDTFET biosensor can be assessed by the drain current sensitivity S_{Drain} [7]; higher S_{Drain} indicates better detection of molecules and can be defined as:

$$S_{Drain} = (I_{Drain}^{Bio} - I_{Drain}) / I_{Drain}$$

Where, I_{Drain} and I_{Drain}^{Bio} are drain currents in the absence of biomolecules and in the presence of biomolecules, respectively. However, S_{Drain} demonstrates the inverse relationship with V_{GS} . Therefore, biasing the device at optimum voltage is also a key factor to attain higher sensitivity. Fig. 8 (a) and (b) demonstrate that the sensitivity of drain current of DDMEDTFET biosensor with the increasing values of dielectric constants and negative charge densities, respectively with respect to the variation in V_{GS} at a fixed $V_{DS} = 0.5$ V. From Fig. 8 (a), it reaches maximum up to 10^7 for a dielectric constant of $k = 7$. While it reaches to 10^6 for dielectric constant of $k = 5$. However, degradation has been observed in S_{Drain} with the increase in the value of negative charge densities as shown in Fig.8 (b). In spite of this degradation, the DDM-EDTFET with significant variation in S_{Drain} predicts its detectability ranging from -1×10^{11} to -1×10^{12} cm $^{-2}$ with both $k = 5$ and 7 . Similarly, Fig. 8 (c) and (d) shows the drain current sensitivity with the increasing values of dielectric constants and negative charge densities, respectively with respect to the variation in V_{DS} at a fixed $V_{GS} = 1.2$ V.

Fig. 8 (c) shows that S_{Drain} reaches to maximum sensitivity of 10^5 for dielectric constant of $k=7$ and 10^4 for dielectric constant of $k=5$. Fig. 8 (d) indicates that the sensing efficiency decreases with the increasing ρ , associated with the biomolecules conjugation.

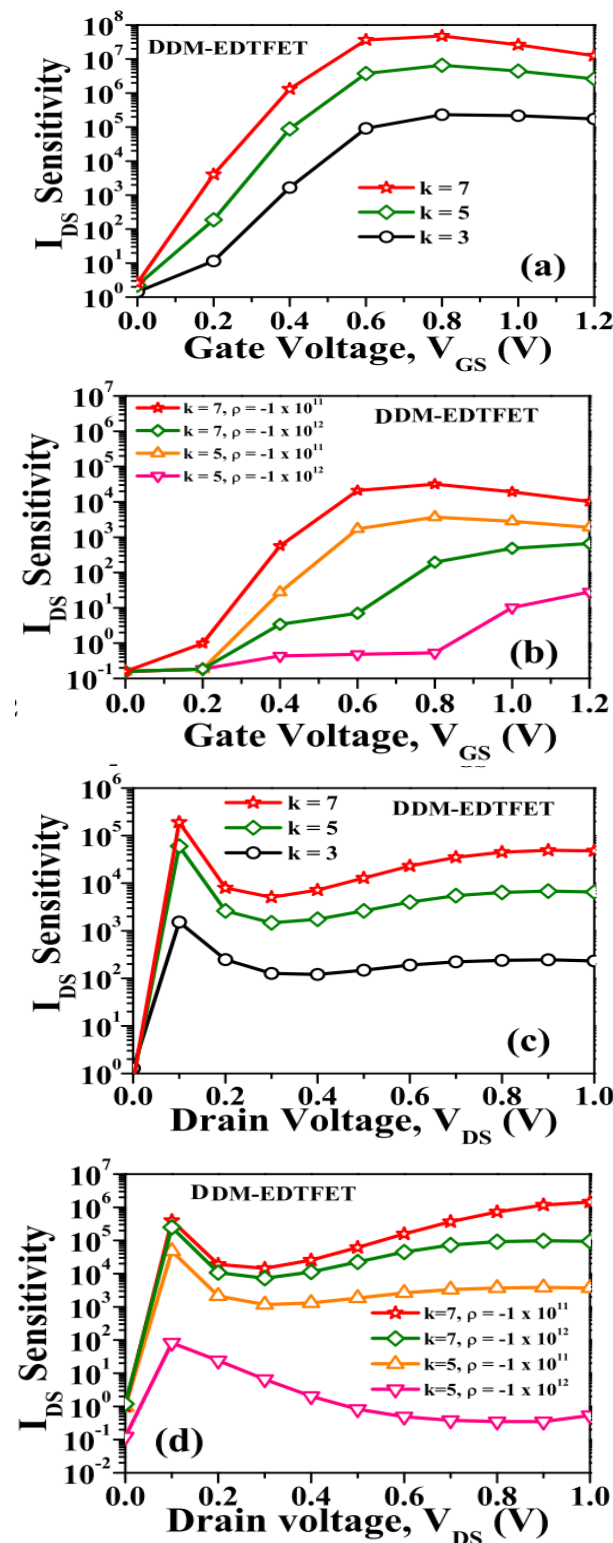


Fig. 8. Drain current sensitivity of DDM-EDTFET with different (a) k but $\rho=0$ and (b) ρ but $k=5$ and 7 ; with V_{GS} variation at a fixed $V_{DS} = 0.5V$. Drain current sensitivity of DDM-EDTFET with different (a) k but $\rho=0$ and (b) ρ but $k=5$ and 7 with V_{DS} variation at a fixed $V_{GS} = 1.2V$.

The observed maximum sensitivity for charged molecules with respect to drain bias are 10^5 . While, with respect to gate bias is 10^4 for $\rho = -1 \times 10^{12}$ at $k=7$. It can be observed from the transfer characteristics of DDMEDTFET based biosensor, the relative change in I_{ON} and V_{th} with increasing values of k is very high. The impacts of charged ($k>1, \rho \neq 0$) as well as charged-neutral ($k>1, \rho = 0$) biomolecules have been also derived from Fig. 6 (a) and (b) as shown in Fig. 9 (a) and (b). More precisely, for sensitivity analysis of DDM-EDTFET, we have considered the following parameters individually as follows: 1) I_{ON} , 2) I_{ON}/I_{OFF} ratio and 3) subthreshold slope (SS). Fig. 9 (a) shows tremendous rise in I_{ON} with changes in k . Also, in the presence of charged biomolecules ($\rho = -10^{12} \text{ cm}^{-2}$) in the cavity, I_{ON} reduces by ten times at low value of ($k=0.5$). We have also shown I_{ON}/I_{OFF} ratio of DDM-EDTFET biosensor with variation in dielectric constant values and negative charge densities in Fig. 9 (b). It can be understood that the increase/decrease in I_{ON}/I_{OFF} ratio with k/ρ is on account of increase/decrease in the value of ON-state current (Fig. 6 (a) and (b)). Also, V_{th} also changes at different dielectric constant with charged biomolecules as can be verified from Fig. 6 (a) and (b). From the sensitivity analysis, it is worthwhile to mention that the effect of biomolecule charge weakens as k increases and is quite sensible for low values of k , thus confirmed the high sensitivity of DDM-EDTFET based biosensor.

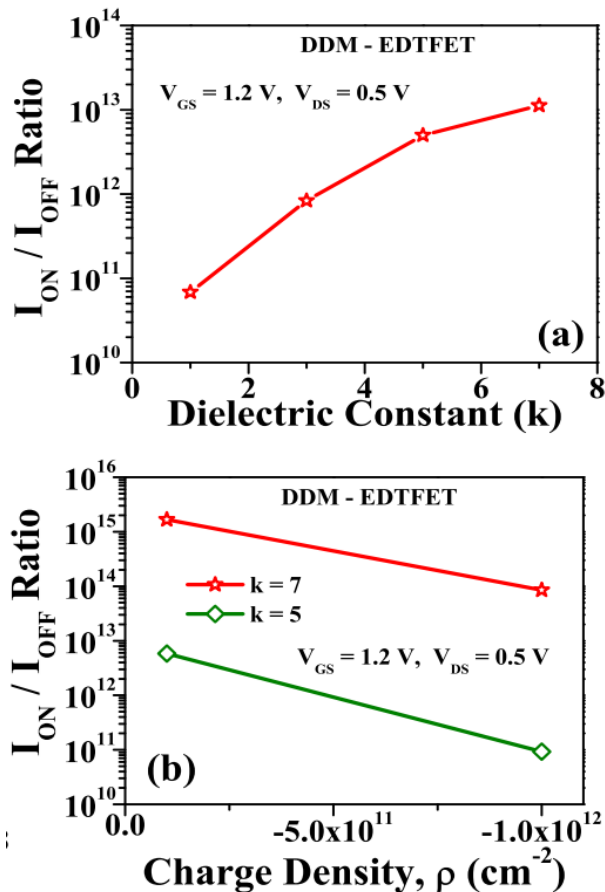


Fig. 9. Impact of charged biomolecules on (a) I_{ON} and (b) I_{ON}/I_{OFF} for a range of dielectric constant ($k=5$, and 7) for a DDM-EDTFET based biosensor at $V_{GS} = 1.2V$ and $V_{DS} = 0.5V$.

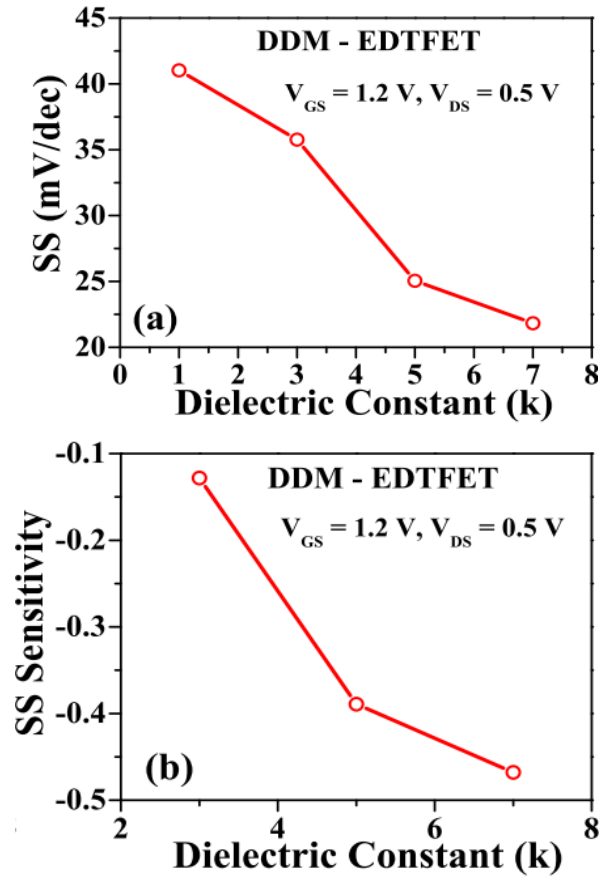


Fig. 10. (a) Subthreshold slope and (b) subthreshold slope sensitivity of the proposed device for $\rho=0$ and dielectric range from $k=1$ to 7 at $V_{GS} = 1.2\text{V}$ and $V_{DS} = 0.5\text{V}$.

In addition, we have also analyzed subthreshold slope for the DDM-EDTFET based biosensor. The subthreshold slope is proportional to gate biasing [21], thus, subthreshold slope is resting on gate biasing that quantify the effectiveness of gate voltage in controlling the channel region. Fig.10 (a) and (b) show the variation in SS with respect to the increasing values of the dielectric constant. It is verified from Fig.10 (a) that with biomolecules conjugation ($k>1$), the gate controlling increases, and which in turn results in reduction in SS. Consequently, a significant improvement in SS sensitivity is achieved with increasing values of k as shown in Fig. 10 (b). Thus, this reduction in SS depicts better detection capability of DDM-EDTFET based biosensor.

D. Effect of parameter variation on device performance
In this section, we have discussed the effect of parameter variation i.e variation in length (L_C) and thickness (t_c) of cavity. Fig.11 (a) demonstrates the transfer characteristics with variation in L_C . It is observed that as L_C increases then no significant improvement in I_{ON} and I_{OFF} is observed with L_C above 15 nm . It is due to the reason that the drain current in TFET depends on tunneling and not in diffusion process. Likewise, Fig.11 (b) shows the variation in cavity thickness on the transfer characteristics of the DDM-EDTFET biosensor.

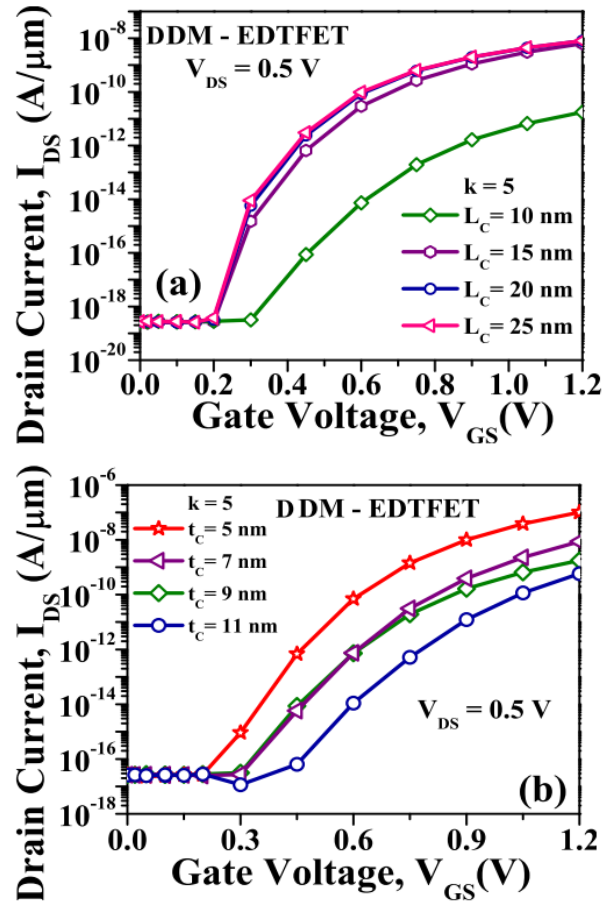


Fig. 11. Effect of variation in (a) the length of cavity (L_C) and (b) the thickness of cavity (t_c) on the transfer characteristics of DDM-EDTFET at $V_{GS} = 1.2\text{V}$ and $V_{DS} = 0.5\text{V}$.

Here, the drain current decreases with the increase in t_c . Since the increment in t_c causes the reduction in the gate field controlling the tunneling of charge carriers and hence the current. This also imposes a requirement for higher gate voltage for better conduction of the device with thicker cavity. Therefore, for better electrical performance of DDM-EDTFET based biosensor, the optimum values are 15nm and 5nm for L_C and t_c , respectively.

IV. CONCLUSION

The performance of dual dielectrically modulated electrostatically doped tunnel-FET has been investigated for biosensing applications in detail. We have explored the underlying physics of DDM-EDTFET and estimated its sensing performance. In addition with significant sensitivity improvement in comparison with other conventional biosensors, the proposed DDM-EDTFET based biosensor offers less fabrication overhead due to the doping-less architecture. Therefore, it is expected to be immune from random dopant fluctuations problems as well as other doping related issues. In this work, the sensing performance of DDM-EDTFET has been evaluated for charged ($k>1$, $\rho\neq 0$) as well as charged-neutral ($k>1$, $\rho=0$) biomolecules conjugation through extensive device-level simulation. In addition, the impact of biomolecule dielectric constant and charge density on both the electrical and sensing

performance of EDTFET based biosensor has been studied. Hence, from the studied, it is confirmed that DDM-EDTFET can be used as an emerging highly sensitive label-free bioequipment in biosensing applications.

V. FUTURE SCOPE

This work will pave the path for the implementation of dual dielectric materials in sensing devices to enhance drain current that results in identification of different charged or neutral biomolecules.

Conflict of Interest. The authors declare that there is no conflict of interest of any sort on this research.

REFERENCES

[1]. Kanungo, S., Chattopadhyay, S., Gupta, P. S., & Rahaman, H. (2015). Comparative performance analysis of the dielectrically modulated full-gate and short-gate tunnel FET-based biosensors. *IEEE Transactions on Electron Devices*, 62(3), 994-1001.

[2]. Narang, R., Reddy, K. S., Saxena, M., Gupta, R. S., & Gupta, M. (2012). A dielectric-modulated tunnel-FET-based biosensor for label-free detection: Analytical modeling study and sensitivity analysis. *IEEE Transactions on Electron Devices*, 59(10), 2809-2817.

[3]. Kim, D. S., Jeong, Y. T., Park, H. J., Shin, J. K., Choi, P., Lee, J. H., & Lim, G. (2004). An FET-type charge sensor for highly sensitive detection of DNA sequence. *Biosensors and Bioelectronics*, 20(1), 69-74.

[4]. Choi, J. M., Han, J. W., Choi, S. J., & Choi, Y. K. (2010). Analytical modeling of a nanogap-embedded FET for application as a biosensor. *IEEE Transactions on Electron Devices*, 57(12), 3477-3484.

[5]. Bergveld, P. (2003). Thirty years of ISFETOLOGY: What happened in the past 30 years and what may happen in the next 30 years. *Sensors and Actuators B: Chemical*, 88(1), 1-20.

[6]. Jhaveri, R., Nagavarapu, V., & Woo, J. C. (2010). Effect of pocket doping and annealing schemes on the source-pocket tunnel field-effect transistor. *IEEE Transactions on Electron Devices*, 58(1), 80-86.

[7]. D. Sarkar and K. Banerjee. (2012). Fundamental limitations of conventional fet biosensors: Quantum-mechanical-tunneling to the rescue. *70th Device Research Conference*. 83-84.

[8]. Im, H., Huang, X. J., Gu, B., & Choi, Y. K. (2007). A dielectric-modulated field-effect transistor for biosensing. *Nature nanotechnology*, 2(7), 430-434.

[9]. Tang, X., Jonas, A. M., Nysten, B., Demoustier-Champagne, S., Blondeau, F., Prévot, P. P., ... & Raskin, J. P. (2009). Direct protein detection with a

nano-interdigitated array gate (MOSFET). *Biosensors and Bioelectronics*, 24(12), 3531-3537.

[10]. De Marchi, M., Sacchetto, D., Frache, S., Zhang, J., Gaillardon, P. E., Leblebici, Y., & De Micheli, G. (2012, December). Polarity control in double-gate, gate-all-around vertically stacked silicon nanowire FETs. In *2012 International Electron Devices Meeting*, (8.4.1-8.4.4). IEEE.

[11]. Boucart, K., & Ionescu, A. M. (2007). Double-Gate Tunnel FET With High- κ Gate Dielectric. *IEEE transactions on electron devices*, 54(7), 1725-1733.

[12]. Lahgere, A., Sahu, C., & Singh, J. (2015). PVT-aware design of dopingless dynamically configurable tunnel FET. *IEEE Transactions on Electron Devices*, 62(8), 2404-2409.

[13]. Sahu, A., Bramhane, L. K., & Singh, J. (2016). Symmetric lateral doping-free BJT: a novel design for mixed signal applications. *IEEE Transactions on Electron Devices*, 63(7), 2684-2690.

[14]. Panchore, M., Singh, J., & Mohanty, S. P. (2016). Impact of channel hot carrier effect in junction-and doping-free devices and circuits. *IEEE Transactions on Electron Devices*, 63(12), 5068-5071.

[15]. Sahu, C., & Singh, J. (2014). Charge-plasma based process variation immune junctionless transistor. *IEEE Electron Device Letters*, 35(3), 411-413.

[16]. Bramhane, L. K., Upadhyay, N., Veluru, J. R., & Singh, J. (2015). Symmetric bipolar charge-plasma transistor with extruded base for enhanced performance. *Electronics Letters*, 51(13), 1027-1029.

[17]. Kumar, M. J., & Janardhanan, S. (2013). Doping-less tunnel field effect transistor: Design and investigation. *IEEE transactions on Electron Devices*, 60(10), 3285-3290.

[18]. Dashiell, M. W., Kalambur, A. T., Leeson, R., Roe, K. J., Rabolt, J. F., & Kolodzey, J. (2002, August). The electrical effects of DNA as the gate electrode of MOS transistors. In *Proceedings. IEEE Lester Eastman Conference on High Performance Devices* (pp. 259-264). IEEE.

[19]. ATLAS Device Simulation Software, Silvaco Int., Santa Clara, CA, USA.

[20]. Chen, Z., Xiao, Y., Tang, M., Xiong, Y., Huang, J., Li, J., ... & Zhou, Y. (2012). Surface-potential-based drain current model for long-channel junctionless double-gate MOSFETs. *IEEE Transactions on Electron Devices*, 59(12), 3292-3298.

[21]. Parihar, M. S., Ghosh, D., & Kranti, A. (2013). Ultra low power junctionless MOSFETs for subthreshold logic applications. *IEEE Transactions on Electron Devices*, 60(5), 1540-1546.

How to cite this article: Bramhane, L. K. Kadbe, P. K. Patil, B. H. Chede, S. D. and Lande, S.B. (2019). Dual Dielectrically Modulated Electrostatically Doped Tunnel-FET for Biosensing Applications. *International Journal on Emerging Technologies*, 10(4): 153-159.